Refractive Indices of Molecules in Vapor and Liquid: Calculations on Benzene

Kristian O. Sylvester-Hvid

Department of Chemistry, Aarhus University, DK-8000 C, Denmark

Kurt V. Mikkelsen*

Department of Chemistry, H. C. Ørsted Institute, University of Copenhagen, DK-2100 Copenhagen Ø, Denmark

Mark A. Ratner

Department of Chemistry, Northwestern University, Evanston, Illinois 60208-3113

Received: August 7, 1998

The refractive indices of benzene in the gas and liquid phase are computed employing a classical electrodynamical treatment of light propagation in continuous media and high level ab initio computations of the relevant molecular properties. We investigate various levels of complexity when deriving expressions relating the microscopic molecular optical properties and the refractive index. Different methods of accounting for the molecular environment within the framework of quantum chemical computations are scrutinized. The fundamental molecular property determining the refractivite index is the polarizability, and dynamic molecular polarizabilities of benzene are adequately computed using a triple-zeta plus double polarization basis; larger basis sets change the computed values by less than 1%. The effects of electronic correlation on the dynamic polarizabililties are discussed. For benzene vapor, computed results for the refractive index agree well with experiment. For liquid benzene, the best agreement with experiment is found using the Lorentz−Lorenz formula with computed gas-phase polarizability. We introduce the isolated molecule classical environment (IMLE) and the iterative self-consistent reaction field approach.

I. Introduction

The refractivity or the refractive index of a material is the most visible result of the optical properties of its constituent components. The importance of refractivity stems not only from its presence in all transparent matter, but also from the wide technological applicability of optical devices, which rely themselves on specific properties of the refractive index, for such applications as optical fibers or optical coatings.

For design of optical devices, where the refractive index is the phenomenon of relevance, effects such as its intensity dependence, dispersion, degree of nonlinearity, and susceptibility to external fields are important. Phenomenological understanding of these effects is available, but first-principles theoretical prediction of these quantities has lagged. Despite the rather advanced quantum chemical tools now available, little effort has been put into quantitative description of refractivity. We address here the issues involved in understanding and theoretically describing the refractive index for the condensed phase, using first principles. When computing the refractive index of any material, ideally one should address the following issues: (i) the relationship between the refractive index and various macroscopic electric and magnetic susceptibilities; (ii) the connection between the microscopic and the corresponding macroscopic susceptibilities; (iii) the computation of the dispersive microscopic molecular susceptibilities, linear or nonlinear; (iv) the incorporation of the molecular environment; (v) the statistical mechanical concerns needed when deriving properties of the bulk; (vi) the time scales for the different degrees of freedom involved in the optical processes. In this preliminary contribution we begin by describing the refractive index as simply as possible, only gradually increase the complexity, then allowing for a rigorous understanding of the various components involved in the computation of refractive indices.

In section II we discuss the classical electrodynamical approach to calculation of refractivety−the approach of preference in the present work. We present a generalization of the equations describing linear materials and subsequently consider the case of pure electric and magnetic responses. Well-established expressions for the refractive index $\mathbf{n}(\omega)$ in isotropic materials are given for two distinct model assumptions: 1. an assembly of isolated polarizable units, 2. an assembly of polarizable units interacting with a dielectric medium. For molecular materials, the polarizable unit can be chosen as a molecule or a cluster of molecules. Here we consider a single molecule only. Thus, in concert with the second model, expressions for $\mathbf{n}(\omega)$ represent different models using classical-electrodynamics to take into account the effects of the molecular environment. This we term the isolated molecule classical environment (IMCE) approach. Alternatively, one may employ the first model (isolated polarizable units) and then incorporate effects of molecular interactions in the quantum description of the polarizable unit, be that a molecule or a cluster of molecules. From a methodological point of view, one should avoid overlapping quantum mechanical and classical models for

* Author to whom correspondence should be addressed.

10.1021/jp983328b CCC: $18.00
Published on Web 10/04/1999

describing molecular interactions. For the part of these interactions, independent of the optical radiation field (referred to as the specific interactions), this separation is straightforward, and such complementary approaches are discussed in section II and section III. However, the effect of the molecular surroundings, as mediated through modulations of the optical radiation field, lack simple quantum mechanical descriptions. This effect, referred to as screening, consequently is treated classically in terms of local field factors. However, using these in the computation of optical bulk properties of pure compounds introduces conceptual problems. Therefore, in section III we present an iterative implementation of the multiconfigurational self-consistent reaction field (MCSCRF) model,[1] the iterative self-consistent reaction field (ISCRF) approach, which circumvents inconsistencies arising from a combined local field factor and MCSCRF model.

Prior to investigating effects of molecular interactions, the reliability of the fundamental computations of dynamical polarizabilities is scrutinized. Thus, extensive vacuum computations of $\alpha(-\omega,\omega)$ for benzene are presented in order to establish a confidence level with respect to choice of basis set and level of correlation. The computational details are given in section IV along with a brief review of ab initio vacuum computations of $\alpha(-\omega,\omega)$ for benzene. Following this, we then present quantum computations modeling the condensed phase, the computational details of which also reside in section IV.

In section V we discuss results of polarizability computations and compare with experimental depolarization data. Our main objective is to learn how the different models of section III describe the refractive index. Examples of different uses of these models are presented in section VI along with comparisons to experiment. Finally, conclusive remarks are given in section VII.

II. Refractive Index

The refractive index $\mathbf{n}(\omega)$ and the dielectric function $\epsilon(\omega)$ can be thought of as macroscopic, frequency dependent properties related through the Maxwell relation:[2,3]

$$\mathbf{n}(\omega) = \epsilon(\omega)^{1/2} \tag{1}$$

The dielectric function shows a variety of characteristics in different frequency regions, with each frequency region being characterized by the response of particular microscopic degrees of freedom. Symbolically, this is often written as

$$\epsilon = \epsilon_{\text{inter}} + \epsilon_{\text{intra}} \tag{2}$$

where the intermolecular contributions arise from translation and rotation of molecules or molecular aggregates, and vibration of molecular aggregates. Intramolecular contributions mainly arise from molecular vibrations and electronic motion. As the frequency of the external perturbation is increased, the slower degrees of freedom freeze such that at optical frequencies or higher, only the electronic subsystem contributes to the dielectric function.

In the present work our concern is the dispersive behaviour of $\mathbf{n}(\omega)$ in the optical frequency range, which is the primary justification for neglecting all but electronic contributions to eq 2. We use classical electrodynamics, and consider the propagation of electromagnetic radiation in a continuum, such that the Maxwell equations provide an appropriate description. On a microscopic level the material is composed of non-polar molecules to which we assign molecular susceptibilities. These are extracted from quantum chemical computations.

A. Fundamental Model. Consider electromagnetic radiation propagating in an infinite medium that we shall take to be homogeneous, nonconducting and without any free charges. The Maxwell fields (the macroscopic average electric, $\mathbf{E}(\mathbf{r}, t)$, and magnetic, $\mathbf{H}(\mathbf{r}, t)$, fields) must then obey the following wave equation[4]

$$\nabla^2\mathbf{E}(\mathbf{r}, t) = \frac{1}{c^2}\frac{\partial^2}{\partial t^2}\{\mathbf{E}(\mathbf{r}, t) + 4\pi\mathbf{P}(\mathbf{r}, t)\} + \frac{4\pi}{c}\frac{\partial}{\partial t}\{\nabla \times \mathbf{M}(\mathbf{r}, t)\}$$

$$\nabla^2\mathbf{H}(\mathbf{r}, t) = \frac{1}{c^2}\frac{\partial^2}{\partial t^2}\{\mathbf{H}(\mathbf{r}, t) + 4\pi\mathbf{M}(\mathbf{r}, t)\} - \frac{4\pi}{c}\frac{\partial}{\partial t}\{\nabla \times \mathbf{P}(\mathbf{r}, t)\} \tag{3}$$

where we have adopted the gaussian system of units.

The wave equations do not constitute a physical model until the macroscopic average polarization, $\mathbf{P}(\mathbf{r}, t)$ and magnetization $\mathbf{M}(\mathbf{r}, t)$ governing the medium have been specified. Assuming, a medium capable of linear responses only, the equations generally read

$$\mathbf{P}(\mathbf{r}, t) = {}^{ee}\chi\mathbf{E}(\mathbf{r}, t) + {}^{em}\chi\mathbf{H}(\mathbf{r}, t)$$

$$\mathbf{M}(\mathbf{r}, t) = {}^{me}\chi\mathbf{E}(\mathbf{r}, t) + {}^{mm}\chi\mathbf{H}(\mathbf{r}, t) \tag{4}$$

and therefore represent a model where electric and magnetic fields are linearly coupled in all possible ways. All four χ tensors are of second rank, and eq 4, therefore, allows for describing the linear response of any anisotropic medium. We consider propagation of plane waves only, assuming a definite state of linear polarization, i.e.

$$\mathbf{E}(\mathbf{r}, t) = \mathbf{E}^0 e^{i(\mathbf{k}\cdot\mathbf{r}-\omega t)}, \quad \mathbf{H}(\mathbf{r}, t) = \mathbf{H}^0 e^{i(\mathbf{k}\cdot\mathbf{r}-\omega t)} \tag{5}$$

Upon insertion of eq 5 and eq 4 into eq 3, the wave equations may be cast into a matrix equation with the following structure

$$\begin{pmatrix}\mathbf{A}_{11} & \mathbf{A}_{12}\\ \mathbf{A}_{21} & \mathbf{A}_{22}\end{pmatrix}\begin{pmatrix}\mathbf{E}\\ \mathbf{H}\end{pmatrix} = \begin{pmatrix}\mathbf{0}\\ \mathbf{0}\end{pmatrix} \tag{6}$$

and with the following identification of the submatrices:

$$\mathbf{A}_{11} = \{(n^2 - 1)\mathbf{1} - 4\pi^{ee}\chi + 4\pi n\mathbf{d}^{me}\chi\}$$

$$\mathbf{A}_{12} = \{4\pi n\mathbf{d}^{mm}\chi - 4\pi^{em}\chi\}$$

$$\mathbf{A}_{21} = \{-4\pi n\mathbf{d}^{ee}\chi - 4\pi^{me}\chi\}$$

$$\mathbf{A}_{22} = \{(n^2 - 1)\mathbf{1} - 4\pi^{mm}\chi - 4\pi n\mathbf{d}^{em}\chi\} \tag{7}$$

For notational convenience we have introduced a matrix

$$\mathbf{d} = \begin{pmatrix}0 & -\hat{k}_z & \hat{k}_y\\ \hat{k}_z & 0 & -\hat{k}_x\\ -\hat{k}_y & \hat{k}_x & 0\end{pmatrix} \tag{8}$$

that has as its off-diagonal elements components of the unit vector $\hat{\mathbf{k}}$, defining the direction of propagation. The index of refraction along $\hat{\mathbf{k}}$ is then defined through $\mathbf{k} = (\omega/c)(n\hat{\mathbf{k}})$. Once all susceptibilities have been specified and a direction of propagation $\hat{\mathbf{k}}$ chosen, the refractive index is determined from

$$\mathrm{Det}\begin{pmatrix}\mathbf{A}_{11} & \mathbf{A}_{12}\\ \mathbf{A}_{21} & \mathbf{A}_{22}\end{pmatrix} = 0 \tag{9}$$

In deriving eq 7, the macroscopic average fields (the Maxwell fields) inside the medium were employed. Note, however, that eq 7 contains no reference to the magnitude of the magnetic and electric fields. Therefore, if the susceptibilities have a molecular origin according to $\chi^{\mathrm{macro}} = N\,\chi^{\mathrm{micro}}$, then the determination of $\mathbf{n}(\omega)$ from eq 7 corresponds to considering a set of noninteracting polarizable molecules, with density N.

On a phenomenological level we can incorporate effects of molecular interactions into the description by considering the notion of a Lorentz effective field. In cases where electric polarization is the predominant effect, we consider an effective electric field to be

$$\mathbf{E}_{\mathrm{eff}} = \mathbf{E} + \mathbf{LP} \tag{10}$$

such that the Maxwell field is corrected with a term proportional to the macroscopic average polarization. The Lorentz tensor[3] is generally written in terms of two contributions

$$\mathbf{L} = \mathbf{F} + \mathbf{T} \tag{11}$$

which model complementary types of molecular interactions. The matrix **F**, called the cavity tensor, corrects the Maxwell field arising from polarization of the medium when considered to be a continuum and one obtains the effective field inside a virtual cavity embedded in the dielectric medium. Information regarding the cavity geometry and the degree of anisotropy of the dielectric medium then is contained in the specific form of **F**. Commonly, the cavity tensor, **F** simply is taken as

$$\mathbf{F} = \frac{4\pi}{3}\mathbf{I} \tag{12}$$

which according to the Lorentz correction[5] mirrors the local field at the center of a virtual, spherical cavity in an isotropic dielectric medium.

The matrix **T** contributes to the local field the discrete part of the molecular environment represented by some configuration of point dipoles (or multipoles). Typically, **T** sums contributions to the local field due to a finite array of point dipoles representing neighboring molecules. In this case the tensor **T** acquires a form such as[6,2]

$$\mathbf{T} = -\lim_{V\to\infty}\sum_{V} r^{-3}(\mathbf{1} - 3r^{-2}\mathbf{rr})\frac{1}{N} \tag{13}$$

As can be seen from eq 10, the effective field depends on the current polarization state of the medium, which again depends on the effective field. Performing the required self-consistent procedure leads to the following effective field, referred to as the internal field[57]

$$\mathbf{E}_{\mathrm{int}} = (\mathbf{1} - \mathbf{L}^{ee}\chi)^{-1}(\mathbf{E} + \mathbf{L}^{em}\chi\mathbf{H}) \tag{14}$$

Rederiving eq 7, using the internal electric field instead of **E**, gives

$$\mathrm{Det}\begin{pmatrix}\mathbf{A}_{11} - (n^2-1)\mathrm{L}^{ee}\chi & \mathbf{A}_{12} - (n^2-1)\mathrm{L}^{em}\chi\\ \mathbf{A}_{21} & \mathbf{A}_{22}\end{pmatrix} = 0 \tag{15}$$

B. Some Simplified Models. In the previous section we formalized a method for calculating $\mathbf{n}(\omega)$. The full generality has been kept so as to allow us to treat any linear optical phenomenon in isotropic, monoaxial or biaxial optical systems. We now specialize to the case of pure isotropic media characterized by

$$\begin{aligned} {}^{ee}\chi &= \langle {}^{ee}\chi\rangle = \mathrm{Tr}({}^{ee}\chi)\\ {}^{mm}\chi &= \langle {}^{mm}\chi\rangle = \mathrm{Tr}({}^{mm}\chi)\\ {}^{em}\chi &= \mathbf{0}\\ {}^{me}\chi &= \mathbf{0} \end{aligned} \tag{16}$$

where $\langle ... \rangle$ denotes the spatial average. A model defined through eq 16 is only appropriate for describing the gas phase and some liquid systems. Typically, such liquids must have a low degree of molecular association and consist of nonpolar molecules.

Invoking the Lorentz correction, the refractive index thus becomes

$$n = \sqrt{\frac{\{3 + 8\pi^{ee}\chi\}\{1 + 4\pi^{mm}\chi\}}{\{3 - 4\pi^{ee}\chi\}}} \tag{17}$$

which in the case of vanishing magnetization reduces to

$$n = \sqrt{\frac{3 + 8\pi^{ee}\chi}{3 - 4\pi^{ee}\chi}} \tag{18}$$

Without the Lorentz correction, the equivalent of eq 17 takes the form

$$n = \sqrt{1 + 4\pi\{{}^{ee}\chi + {}^{mm}\chi\} + 16\pi^{2}{}^{ee}\chi^{mm}\chi} \tag{19}$$

and in the case of vanishing magnetization, we retrieve the most simple equation for calculating the refractive index:

$$n = \sqrt{1 + 4\pi^{ee}\chi} \tag{20}$$

III. Molecular Environment

In section II we saw that the influence of the molecular surroundings on $n(\omega)$ may be modeled through the notion of an internal field. By its definition, however, the internal field does not directly address the molecular origin of the continuous medium. To shift the focus to the molecular properties we imagine a molecule, described by an average polarizability, α, at the center of a Lorentz cavity. The internal field E_{i} then is the field experienced by this molecule, giving a microscopic polarization, $p = \alpha E_{\mathrm{i}}$. Taking the molecule in the cavity as a representative subunit of the bulk with the macroscopic polarization, $P = \chi E = N\alpha E_{\mathrm{i}}$, together with the Lorentz correction,[5] gives a macroscopic susceptibility in terms of the molecular polarizability[6]

$$\chi = \frac{3N\alpha}{3 - 4\pi N\alpha} \tag{21}$$

Upon insertion of eq 21 in eq 20, the Lorenz−Lorentz equation[7,5] results

$$n = \sqrt{\frac{3 + 8\pi N\alpha}{3 - 4\pi N\alpha}} \tag{22}$$

which, on the other hand, also results from setting $\chi = N\alpha$ in eq 18.

The use of local field factors arises since measured optical properties relate to the Maxwell field, whereas each molecule is subject to the internal field. The fields are related as $E_i = fE$, such that the macroscopic susceptibility becomes

$$\chi = Nf^{L}(n)\alpha = N\left(\frac{n^2+2}{3}\right)\alpha \tag{23}$$

where f^L is the local field factor appropriate in the Lorentz model at optical frequencies in the case of linear polarization.

The form of eq 23 allows interpreting $f^L\alpha$ as an effective molecular polarizability, corrected for effects of the surroundings. Hence, insertion of eq 23 in eq 20 should yield eq 22, as indeed is the case.

Clearly, the Lorenz−Lorentz equation can be approached in several ways, differing in their emphasis on the molecularity of the medium. Note, however, that in none of these approaches reference as to the nature of α is made. In some approaches, where eq 22 and its generalizations are employed,[8−12] the implicit assumption is that $\alpha = \alpha^{vac}$. This cannot be the case, however, since the macroscopic polarization is a consequence of the external field (for nonpolar molecules and $T = 0$), and in the absence of such there can be no internal field. Accordingly, the Lorentz internal field accounts only for molecular interactions as mediated through the optical field. All other molecular interactions, occuring irrespective of the external field, must therefore be included in the calculation of α, which is referred to as α_{sol}. Hence, we write the refractive index as

$$n = \sqrt{1 + 4\pi N\alpha^{eff}} \tag{24}$$

where $\alpha^{eff} = f^L(n)\alpha^{sol}$. The determination of α_{sol} may then follow various IMCE methods, as covered by Böttcher[2] or recently treated by Wortmann et al.[13] Alternatively, environmental effects are incorporated into the quantum mechanical derivation of α_{sol}, as we shall consider below. In case we neglect the specific molecular interactions, that is to say $\alpha_{sol} = \alpha^{vac}$, eq 24 becomes equal to eq 22. Neglecting molecular interactions all together leads to

$$n = \sqrt{1 + 4\pi N\alpha^{vac}} \tag{25}$$

as appropriate only for describing the gas phase.

A. An Iterative Implementation of the MCSCRF Model. Having considered the consequences of the Lorentz internal-field correction, we now outline a quantum mechanical treatment of a molecule in a spherical cavity, surrounded by an isotropic dielectric medium.

We use the current implementation of the equilibrium MCSCRF method[1] in the DALTON program.[14] This involves solving the electronic structure for a molecular state coupled to a polarizable, dielectric continuum in the presence of a time dependent radiation field. Such computations require both the specification of the radius of the cavity R_{cav} and the dielectric constant of the surrounding dielectric medium. Using response theory,[1,15−18] we evaluate linear molecular optical properties for the MCSCRF state as obtained above. The MCSCRF wave function depends on the dielectric constant of the surrounding medium. Therefore, the molecular optical properties are also functions of the dielectric constant. Thus, with respect to our efforts to determine $n(\omega)$ from first principles, the MCSCRF method is useful only if implemented iteratively. Such a procedure is initiated by calculating the optical dielectric constant using the polarizability for the gas phase molecule and an appropriate relation from section III. An MCSCRF computation is then performed using this dielectric constant as input which results in an improved molecular polarizability. Subsequently, a new dielectric constant is derived and used as input in the following MCSCRF computation. This iterative procedure, as illustrated in Figure 4, thus involves transitions between the microscopic and macroscopic regimes: the MCSCRF procedure yields molecular optical properties based on optical bulk susceptibilities, which, on the other hand, are derived from microscopic properties using a model from section III. The result of this ISCRF procedure is a set of optical properties (microscopic and macroscopic) determined self-consistently from first principles.

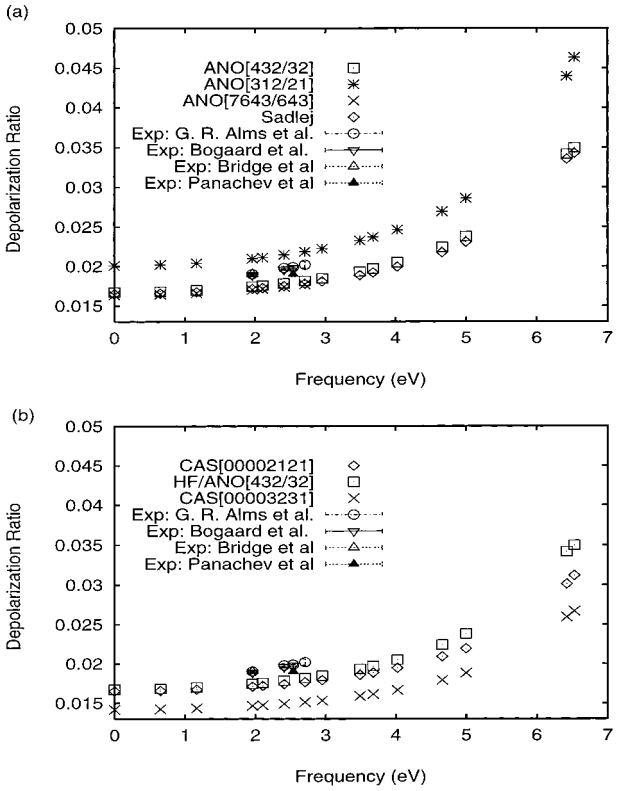

Figure 1. Dispersion of theoretical depolarization ratios compared with experimentally determined depolarization ratios (Alms et al.,[54] Bogaard et al.,[55] Bridge et al.,[46] and Panachev et al.[56]). (a) Theoretical depolarization ratios based on HF polarizabilities computed using basis sets as indicated in the legend. (b) Depolarization ratios derived from CAS polarizabilities and corresponding HF polarizabilities.

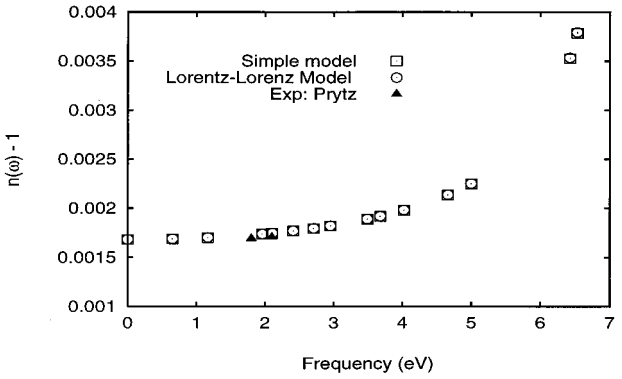

Figure 2. The refractive index of benzene at 293.15 K and 1 bar as a function of frequency computed within the simple (eq 25) and the Lorentz−Lorenz (eq 22) model for refractivities. Refractivities calculated from HF polarizabilities and densities from a virial equation[47] applicable to gas phase benzene. Experimental determinations of the refractive index of benzene vapor[49] are also shown.

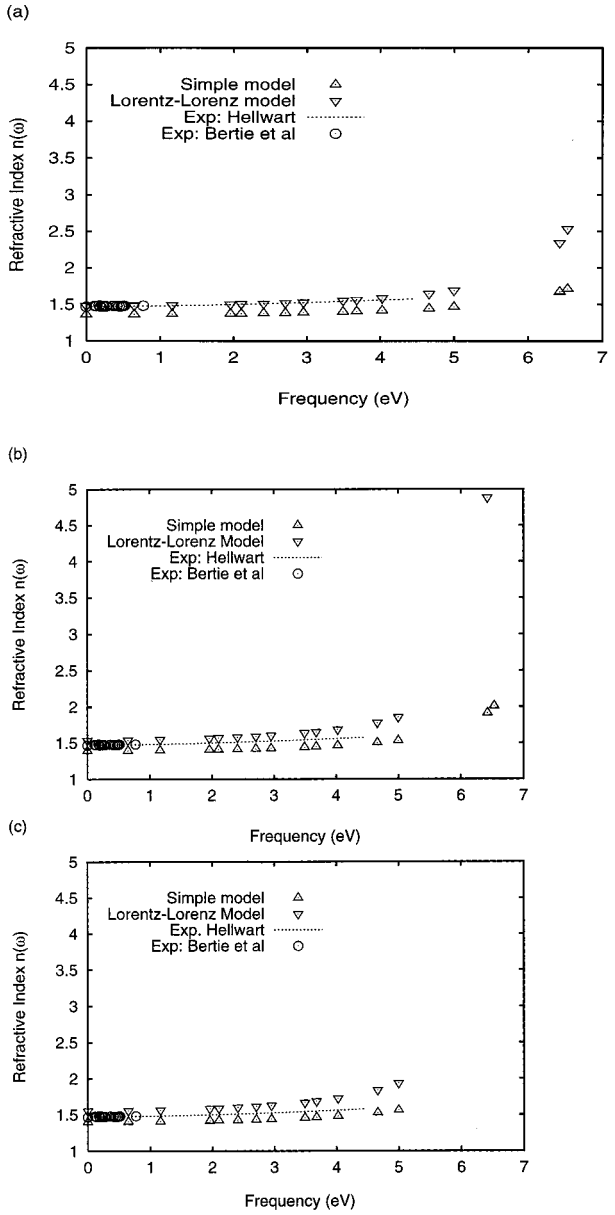

Figure 3. The refractive index of liquid benzene at $\rho = 0.8765$ g/cm, 293.15 K as a function of frequency. Values have been derived according to the simple (eq 25) and the Lorentz−Lorenz (eq 22) model for refractivities. In (a) HF polarizabilities from vacuum computations have been employed, as opposed to (b) were ISCRF polarizabilities were employed using $\epsilon = 1 + 4\pi - \langle\alpha\rangle$. (c) Depicts the same situation as in (b) but for the ISCRF method based on $\epsilon = (3 + 8\pi - \langle\alpha\rangle)/3 - 4\pi - \langle\alpha\rangle)$. Also shown are experimental refractivities corresponding to the IR region and the UV−VIS region.

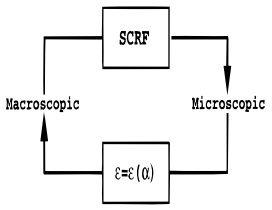

Figure 4. Schematic representation of the ISCRF method. The SCRF model gives molecular polarizabilities from the dielectric function, whereas the other model connects the dielectric function with microscopic optical susceptibilities.

IV. Computation of Polarizabilities

A. Vacuum Polarizabilities for Benzene. Several ab initio studies of the polarizability tensor of benzene have been performed using various formalisms. The finite field (FF) method has been applied to either Hartree−Fock energies,[19−21] MP-2,[21,22] or approximate MP-4[23] correlation corrected Hartree−Fock energies. These studies only dealt with static polarizabilities. Alternatively, static polarizabilities have been computed either by the coupled perturbed Hartree−Fock (CPHF) method, with[21,24] or without[21,25,26] MP-2 correlation included, or by the derivative Hartree−Fock method.[27]

Some studies to date have dealt with effects of electron correlation[21−24,28] but only in one of these[29] were dynamic polarizabilities computed. In the latter case these were derived using a sum over states type expression and the coupled cluster effective Hamiltonian (CCEH) approach, implemented at the SD level of theory. Finally, dynamic but uncorrelated polarizabilities were obtained using time-dependent Hartree−Fock (CPHF) theory[30] or through the random phase approximation (RPA).[31] Table 1 summarizes what we believe the individual authors took as their best theoretical estimates of the polarizability tensor of benzene using uncorrelated theory. Table 2 displays similar results using methods accounting for electron correlation.

It is well-established that the computation of molecular polarizabilities makes special requirements as to the polarization and diffusiveness of the basis set employed. Consequently, several ways of augmenting existing, either energy or geometry optimized basis sets have been explored.

Only few of these, however have been successful as to simultaneous convergence of more than a single molecular property, i.e., the polarizability. For example, on reoptimizing a basis set to yield an improved description of α, the validity is put to question if the Hartree−Fock energy increases,[25] if at all investigated. Also, in studies concerned with effects of electron correlation, results would appear more conclusive if consensus existed as to the Hartree−Fock limit of the benzene polarizability.

B. ANO Polarizabilities of Benzene Using Linear Response Theory. Thus motivated we computed ab initio polarizabilities of benzene using MCSCF linear response theory. This allows the evaluation of dynamic polarizabilities, both at the Hartree−Fock level and at various levels of correlation. However, to assess the importance of electron correlation, we first exhausted the one-electron space, systematically, through the use of the ANO basis sets by Widmark et al.[32,33] Subsequently, we imposed a correlated description, for which the ANO basis actually was designed.

Almlöf et al.[34] have suggested certain ways of enlarging the ANO basis set to maintain a balanced description of the entire orbital space. Following such guidelines gives an expansion as illustrated in Figure 5. The numbers in parantheses designate how the totally decontracted ANO set, 14s9p4d/8s4p (or 14s9p4d3f/8s4p3d in case of added polarization functions) has been contracted for carbon and hydrogen, respectively.

A certain level of electron correlation in the MCSCF procedure is specified by choosing a complete active space (CAS) according to the natural occupation numbers obtained from MP-2 computations. With the molecular symmetry and orientation as described below, the specification of the active orbitals refers to the following symmetry species: a_g, b_{3u}, b_{2u}, b_{1g}, b_{1u}, b_{2g}, b_{3g}, and a_u. In this way, the smallest CAS, denoted [00002121] in Table 6 and 7, corresponds to the π-space in a minimal basis computation. Extending this CAS to include a larger fraction of the $\pi-\pi$ correlation gives [00003231] with two correlating orbitals for each occupied.

The [432/32] basis set was employed in all CAS computations such that the smaller CAS includes 104 determinants whereas

TABLE 1: Selected ab Initio SCF Polarizabilities for Benzene[e]

	$\nu = 0$ au		$\nu = 0.0774$ au					
basis set	α_{xx}	α_{zz}	α_{xx}	α_{zz}	r_{CC}	r_{CH}	ref	method[a]
Sadlej	77.54	44.54	80.81	45.78	1.384	1.072	[29]	
6-31G (sd, sp)	79.01	42.17			1.395	1.085	[23]	FF
Sadlej	79.47	45.45	82.95	46.74	1.395	1.085	[31]	RPA[b]
6-31G+G(3d, 3p)	77.51[c]	44.69					[24]	CHF
C:TZ2P H:TZP	76.94	41.36			1.397	1.084	[27]	DHF
DZPP	73.5	41.4					[20]	FF
4-31G (C: p, d)	74.16[d]	39.48	77.27	40.63	1.384	1.072	[30]	TDHF
[14s8p4d/9s6p4d] [8s3p/6s3p]	79.14	45.28			1.395	1.085	[26]	CHF
Sadlej	79.46	45.45			1.395	1.085	[25]	CHF
4-31G (C: p,d)	74.21	39.47			1.384	1.072	[22]	FF
Dunnings DZ	71.87[a]	32.02			1.4	1.09	[19]	FF
3-21G (C: p, d)	73.82[d]	38.39					[21]	CPHF
3-21G (C: p, d)	73.82[d]	38.46					[21]	FF
ANO (C: p, d)	78.29	43.72			1.3902	1.0862	[28]	RPA

[a] These methods are discussed in section IV. [b] The polarizabilities were calculated using the Cauchy moments given in the paper with k ranging from 1 to 4. [c] Converted from MKSA units according to 1 au = 1.6488×10^{-41} C^2 m^2 J^{-1}. [d] Converted from electrostatic units according to 1 au = 1.48189×10^{-25} cm^3. [e] The values listed are those that the individual authors took as their best estimates. Polarizabilities are displayed in atomic units and bond lengths in angstroms.

TABLE 2: Selected ab Initio Correlated Polarizabilities for Benzene Computed in Previous Studies[c]

	$\nu = 0$ au		$\nu = 0.0774$ au					
basis set	α_{xx}	α_{zz}	α_{xx}	α_{zz}	r_{CC}	r_{CH}	ref	method
6-31G (sd, sp)	79.50	42.24			1.394	1.085	[23]	SDQ-MP4
Sadlej	82.02	45.19	85.49	46.42	1.384	1.072	[29]	CCSD-EH
4-31G (C: p, d)	76.02	41.28			1.384	1.072	[22]	FF MP-2
3-21G (C: p, d)	75.64[a]	40.15					[21]	FF MP-2
Dunnings DZ	71.14	37.63			1.3902	1.0862	[28]	MCSCF[b]

[a] Converted from electrostatic units according to 1 au = 1.48189×10^{-25} cm^3. [b] Cubic response theory using a CAS[00004242]. [c] The values listed are those that the individual authors took as their best estimates. Polarizabilities are displayed in atomic units and bond lengths in angstroms.

TABLE 3: Polarizabilities, α_{xx} (au) at Seven Frequencies, Computed at the Hartree−Fock Level Using Various Levels of Contraction of the ANO Basis Set

λ(nm)	∞	1907	1064	632.8	589	514.3	457.9
ν(au)	0	0.0239	0.0428	0.0720	0.0774	0.0886	0.0995
3s2p1d/2s1p	75.022	75.296	75.915	77.643	78.080	79.117	80.317
4s3p2d/3s2p	79.615	79.923	80.619	82.565	83.057	84.229	85.585
4s3p2d1f/3s2p1d	79.791	80.101	80.799	82.752	83.246	84.422	85.783
5s4p3d/4s3p	79.703	80.015	80.717	82.684	83.182	84.367	85.741
5s4p3d2f/4s3p2d	79.671	79.981	80.682	82.645	83.142	84.325	85.695
6s5p4d/5s4p	79.739	80.050	80.755	82.726	83.225	84.413	85.791
6s5p4d3f/5s4p3d	79.712	80.023	80.726	82.693	83.190	84.376	85.750
7s6p4d/6s4p	79.720	80.032	80.736	82.708	83.207	84.396	85.774
7s6p4d3f/6s4p3d	79.695	80.006	80.709	82.675	83.172	84.357	85.731

TABLE 4: Polarizabilities, α_{zz} (au) at Seven Frequencies, Computed at the Hartree−Fock Level Using Various Levels of Contraction of the ANO Basis Set

λ(nm)	∞	1907	1064	632.8	589	514.3	457.9
ν(au)	0	0.0239	0.0428	0.0720	0.0774	0.0886	0.0995
3s2p1d/2s1p	39.792	39.868	40.041	40.513	40.630	40.906	41.220
4s3p2d/3s2p	45.109	45.217	45.459	46.127	46.293	46.685	47.134
4s3p2d1f/3s2p1d	45.461	45.571	45.819	46.503	46.673	47.075	47.534
5s4p3d/4s3p	45.323	45.436	45.690	46.391	46.565	46.977	47.448
5s4p3d2f/4s3p2d	45.376	45.490	45.744	46.446	46.621	47.034	47.506
6s5p4d/5s4p	45.498	45.613	45.872	46.587	46.765	47.186	47.668
6s5p4d3f/5s4p3d	45.445	45.560	45.817	46.529	46.707	47.126	47.606
7s6p4d/6s4p	45.537	45.653	45.913	46.629	46.808	47.230	47.714
7s6p4d3f/6s4p3d	45.476	45.591	45.849	46.561	46.739	47.159	47.640

the larger includes 1788. Regarding the geometry of benzene, we use $r_{CC} = 1.395$ Å and $r_{CH} = 1.085$ Å,[35] close to the more frequent experimental values: $r_{CC} = 1.397$ Å and $r_{CH} = 1.084$ Å,[36] and $r_{CC} = 1.3964$ Å and $r_{CH} = 1.0831$ Å.[37]

All computations were carried out with the cartesian origin coinciding with the center of mass and the highest possible Abelian symmetry (D_{2h}). The molecule was oriented with the molecular plane coincident with the cartesian xy plane and with two carbon atoms along the y axis.

C. Condensed Phase Polarizabilities. The ISCRF approach is used to describe liquid benzene using the MCSCRF procedure iteratively. The MCSCRF procedure was originally devised to

TABLE 5: Hartree−Fock Polarizabilities as Obtained for Different Basis Sets, Geometries, and Integral Representation[b]

	$\nu = 0$ au		$\nu = 0.0774$ au			
basis set	α_{xx}	α_{zz}	α_{xx}	α_{zz}	r_{CC}	r_{CH}
Sadlej	77.531	44.541	80.373	45.615	1.3840	1.0720
4-31G (C: p, d)[a]	74.183	39.443	77.267	40.640	1.3840	1.0720
Sadlej[a]	79.461	45.453	82.942	46.736	1.3950	1.0850
Sadlej	79.468	45.227	82.948	46.510	1.3950	1.0850

[a] Integrals evaluated in Cartesian basis. [b] Polarizabilities are displayed in atomic units and bond lengths in angstroms.

TABLE 6: MCSCF Polarizabilities, α_{xx} (au) Computed for Different Types of CAS Using the [432/32] Basis Set[a]

λ(nm)	λ(nm)∞	λ(nm)1907	λ(nm)1064	λ(nm)632.8	λ(nm)589	λ(nm)514.3	λ(nm)457.9
ν(au)	ν(au)0	ν(au)0.0239	ν(au)0.0428	ν(au)0.0720	ν(au)0.0774	ν(au)0.0886	ν(au)0.0995
00002121	74.283	74.525	75.070	76.581	76.959	77.856	78.884
00003231	76.434	76.707	77.332	79.035	79.467	80.492	81.675

[a] The individual CAS is specified by the number of active orbitals for the following symmetry species; a_g, b_{3u}, b_{2u}, b_{1g}, b_{1u}, b_{2g}, b_{3g}, and a_u, respectively.

TABLE 7: MCSCF Polarizabilities, α_{zz} (au) Computed for Different Types of CAS Using the [432/32] Basis Set[a]

λ(nm)	λ(nm)∞	λ(nm)1907	λ(nm)1064	λ(nm)632.8	λ(nm)589	λ(nm)514.3	λ(nm)457.9
ν(au)	ν(au)0	ν(au)0.0239	ν(au)0.0428	ν(au)0.0720	ν(au)0.0774	ν(au)0.0886	ν(au)0.0995
00002121	42.273	42.359	42.554	43.084	43.216	43.524	43.874
00003231	45.618	45.735	45.996	46.717	46.897	47.321	47.806

[a] The individual CAS is specified by the number of active orbitals for the following symmetry species; a_g, b_{3u}, b_{2u}, b_{1g}, b_{1u}, b_{2g}, b_{3g}, and a_u, respectively.

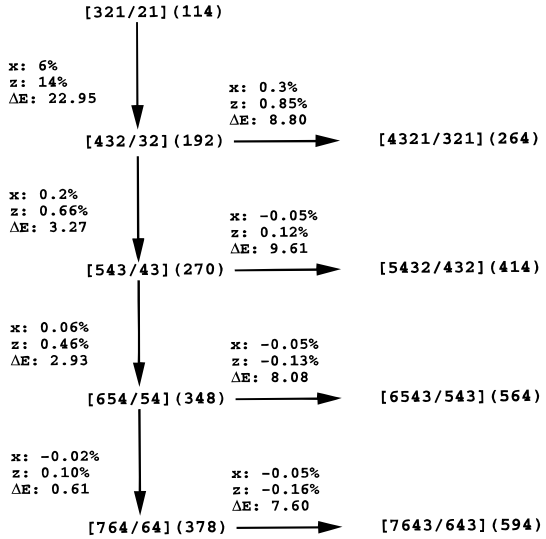

Figure 5. Maximum changes in polarizability components of Benzene, calculated at the HF level, on expansion of the ANO basis set. Vertical arrows correspond to decontraction and horizontal arrows to addition of polarization functions. Also given is the change in the Hartree−Fock energy (10^{-3} au) and the numbers of contracted orbitals. The number of primitive functions for the left row is 486 and 702 for the polarization augmented row.

model molecular properties of a molecule in infinite dilution (such that the dielectric constant is unaffected by the presence of the solute). Here, we consider the benzene molecule solvated by benzene and accordingly, the assumption of infinite dilution breaks down, hence the iterative update of $\epsilon(\omega)$.

Further, we consider the ISCRF procedure at the Hartree−Fock level only, noting that extension of SCRF to MCSCRF is straightforward, being merely a question of computational resources. The individual SCRF computations, one for each frequency of $\epsilon(\omega)$, were all performed using the [432/32] basis set. In Table 8 some representative polarizabilities for successive iterations show the rapid convergence of the ISCRF procedure.

For reasons of comparison, the same geometry was used as for the vacuum computations, with the benzene molecule placed with its center of mass at the center of the spherical cavity of radius $R_{cav} = 3.680$ Å.

We note that the cavity parameter introduces an element of arbitrariness in the (MC)SCRF method. Here, however, we simply comply with the common convention and choose R_{cav} as the distance from the center of mass to the outermost atom plus the van der Waals radius of this atom.

Finally, the multipole expansion of the molecular charge distribution includes charge moments up to $l = 10$ which was shown to give an appropriate representation of the charge distribution.

V. Results and Discussion: Gas Phase Polarizabilities

A. Hartree−Fock Level. Results of the basis set investigation are displayed in Tables 3 and 4. On decontraction from [321/21] to [432/32] α_{xx} generally increases by ∼6% and α_{zz} by ∼14%. Adding polarization functions yields [4321/321], and α_{zz} and α_{zz} increase by ∼0.3% and ∼0.8%, respectively. Further decontraction of the [432/32] set results in small increases of ∼0.2% and ∼0.6% for α_{zz} and α_{zz}.

In Figure 5 we illustrate general trends of this decontraction/expansion process. It is seen that decontraction generally affects α_{zz} more than α_{xx}, which then converges faster than α_{zz}. Also, augmentation with polarization functions has a more pronounced effect on α_{zz}, in accordance with conclusions of others:[19,20] α_{zz} is the more difficult component to describe.

If changes of less than ∼0.2% in the polarizabilities are taken as insignificant fluctuations, from Figure 5 we learn that addition of polarization functions is without effect for basis sets larger than [432/32]. However, it takes decontraction up to [654/54] to obtain convergence for α_{zz}. It appears then that the description of α definitely requires polarization functions on carbon, but that residual improvements are obtained through increased flexibility in the diffuse part of the basis set. Thus, inclusion of *f* functions is of secondary importance, as also anticipated by the choice of basis sets in most previous studies.

TABLE 8: Average Polarizabilities, $\langle\alpha\rangle$ (au) at Four Representative Frequencies, Computed at Successive Iterations during the Iterative Implementation of the ISCRF Procedure[a]

λ(nm)	∞	514.259	265.986	192.983
ν(au)	0	0.08860	0.17130	0.23610
vacuum	68.113	71.714	86.506	143.148
1. iteration	74.208	78.768	98.564	196.809
2. iteration	74.578	79.232	99.633	208.208
3. iteration	74.600	79.262	99.723	210.292
4. iteration	74.601	79.264	99.730	210.662
5. iteration	74.601	79.264	99.731	210.728
6. iteration	74.601	79.264	99.731	210.739

[a] The dielectric constant is updated according to $\epsilon = 1 + 4\pi N \langle\alpha\rangle$.

TABLE 9: Hartree−Fock and CAS Predictions of the Three Lowest Singlet Excitations Observed Experimentally for Gas Phase Benzene[a]

	B_{2u}[b] B_{1u}[c]	B_{3u}[b] B_{2u}[c]	$B_{3u} + B_{2u}$[b] E_{1u}[c]	Oscillator strengths velocity-length
HF/ANO[3s2p1d/2s1p]	(5.90)	(5.84)	7.55	0.7209-0.7213
HF/ANO[4s3p2d/3s2p]	(5.87)	(5.80)	7.43	0.7527-0.7447
HF/ANO[4s3p2d1f/3s2p1d]	(5.86)	(5.81)	7.42	0.7415-0.7444
HF/ANO[5s4p3d/4s3p]	(5.85)	(5.79)	7.36	0.7115-0.7081
HF/ANO[5s4p3d2f/4s3p2d]	(5.84)	(5.80)	7.35	0.6936-0.6938
HF/ANO[6s5p4d/5s4p]	(5.85)	(5.79)	7.31	0.6036-0.6017
HF/ANO[6s5p4d3f/5s4p3d]	(5.84)	(5.80)	7.31	0.5967-0.5977
HF/ANO[7s6p4d/6s4p]	(5.85)	(5.79)	7.24	0.3995-0.3973
HF/ANO[7s6p4d3f/6s4p3d]	(5.84)	(5.80)	7.25	0.4074-0.4069
CAS[00002121]	(7.14)	(4.64)	7.93	0.698-0.6933
CAS[00003231]	(6.78)	(4.75)	7.57	0.667-0.664
observed states[d]	$\tilde{A}$		$\tilde{B}$	$\tilde{C}$
ref 52	6.05−6.70		4.64−5.46	6.81−7.29
ref 53	6.0348−6.204		4.787−4.902	6.866

[a] The corresponding transition moments to the excitation energies given in parenthesis vanish due to the D_{2h} symmetry. In the CAS computation the [432/32] basis set was employed. [b] Symmetry of excited state in D_{2h}. [c] Symmetry of excited state in D_{6h}. [d] The experimental excitation energies are given as the origin and the maximum of the absorption band, respectively.

To extend the comparisons between our determinations of α and previous studies, we performed computations using other geometries, integral representations and basis sets, as displayed in Table 5. Adopting the geometry of Perrin et al.[22] and using the Sadlej basis set,[38] static polarizabilities quoted by Stanton[29] (see Table 1) are reproduced. However, for the corresponding dynamic polarizabilities there seems to be some discrepancy. Comparing the static polarizabilities obtained by Perrin et al. and Shashi et al.[30] using the (*pd*) augmented 4-31G basis set, it appears that TDHF and FF give almost equivalent polarizabilities. However, to reproduce these results and the additional frequency dependent numbers by Shashi, we need to perform the response computations using cartesian integral representation. Analogously, the Sadlej polarizabilities of Lazzeretti[26,31] computed at our geometry are reproduced only if evaluating integrals in the Cartesian basis. Apart from the dynamic polarizabilities quoted by Stanton, different computational schemes produce almost identical numbers (see also ref 21), when taking account of differences due to choice of integral representation. It is unfortunate, however, that the latter has been given no attention since the lack of such differences is indicative of the HF limit. From Table 5 we learn that for basis sets of Sadlej quality effects of integral representation may amount to ~0.5%.

To assess if our ANO polarizabilities are close to the HF limit, we consider the convergence of α in conjunction with related molecular properties. From Figure 5 it appears that, when α converges, the Hartree−Fock energy still improves on expansion of the basis. This leads us to believe that expansion beyond [764/64], most likely, will leave α unaltered. From Table 9 we see that excitation energies (computed as poles of the response function) for the $^1B_{1u}$ and $^1B_{2u}$ states converge quickly, whereas it takes decontraction up to [764/64] in order for the $^1E_{1u}$ excitation energy to converge. For the $^1B_{1u}$ and $^1B_{2u}$ states, these values are within ~0.7% of the high level RPA values of a recent study,[39] whereas the $^1E_{1u}$ excitation energy is ~3% off.

Considering differences between the two representations of the oscillator strengths for the allowed transition to $^1E_{1u}$ (as also given in Table 9) reveals no convergence. On the other hand, the two representations yield very similar numbers, an agreement much better than in ref 39. Although we attain convergence in α, the above excludes anything but a tentative estimate of the HF limit: sets such as [764/64] or larger should give result close to the HF limit.

A qualified estimate of the HF limit of α has been attempted by Lazzeretti et al.[26] who arrived at $\alpha_{xx} = 79.4$ au and $\alpha_{zz} = 46.9$ for the static limit. From Table 3, it appears that our calculations for α_{xx} are approaching a value of 79.7 au, thus slightly higher than Lazzeretti et al. In contrast, 45.5 au for α_{zz} (Table 4) is significantly lower than their estimate. The latter descrepancy is far too large to be ascribed to different uses of integral representation, assuming that neither Lazzeretti et al. nor we have attained the HF limit.

For all practical purposes we concluded that the [432/32] set, composed of 192 contracted functions, represented the best compromise between tractability and accuracy. In terms of α it is comparable to the Sadlej basis set of similar size, which generally is accepted as a high quality polarization basis set. Therefore, all further investigations were performed with this set unless otherwise stated.

B. Effect of Electron Correlation. Comparison of Tables 1 and 2 reveals that all studies but one[28] concerned with electron

correlation reach the same conclusion: correlation increases α. In contrast, from Tables 6 and 7 we learn that CAS computations, limited to the π subspace, generally result in a lower α relative to the HF result, being most pronounced at high frequencies. For [00002121], α_{xx} decreases with ∼8% and α_{zz} with ∼7%. The effect is less pronounced for [00003231] where α_{xx} decrease with ∼5% and α_{zz} is rather unaffected. In case of the [00003231] CAS, a similar decrease in α was computed by Norman et al.,[28] although with a smaller basis set. Expanding the π CAS to [00004242], as recommended by Roos et al.,[40] was hampered by convergence problems for the [432/32] set. According to Norman et al.,[28] however, this does not alter the above conclusion. Also, we find that the dispersion is decreased when correlation is introduced, as is most evident for [00002121], with a ∼2 au decrease in α_{zz} and ∼0.4 au decrease in α_{zz}. The description of excitation energies for the dipole forbidden transitions ($^1A_{1g} \rightarrow {}^1B_{2u}$) and ($^1A_{1g} \rightarrow {}^1B_{1u}$) is improved by correlation as seen from Table 9. The latter transition and especially the allowed ($^1A_{1g} \rightarrow {}^1E_{1u}$) still overestimate experiments, however. Such trends are generally accepted for MCSCF excitation energies and arise because dynamic correlation is poorly accounted for in CAS computations.[28,40−42] Better agreement is obtained with methods which also account for the dynamic correlation (refs 39 and 43 and references therein). For example, second-order perturbative schemes, based on CAS wave functions, significantly improve CAS excitation energies.[40,42] This may indicate that the decrease in α observed for CAS computations is due to insufficient accounting of dynamic correlation. The increase in α seen for MP2 corrected HF computations thus indicates that dynamic correlation has an effect on α which is opposite of the effect of static correlation.

C. Comparisons with Experiment. The Cotton−Mouton effect or the temperature dependence of the Kerr effect both lead to polarization anisotropies.[44,45] Neither, however, offers a unique determination of the anisotropy. Using the Cotton−Mouton effect requires additional information on the magnetic anisotropy, and in the case of the Kerr effect, static polarization anisotropies must be determined. Alternatively, depolarization measurements in concert with refractivity measurements have been used for determining polarization anisotropies.

The classical expression for the depolarization ratio is given by[46]

$$\rho_v = \frac{I_v^{\mathrm{h}}}{I_v^{\mathrm{v}}} = \frac{\gamma^2}{15\alpha^2 + \frac{4}{3}\gamma^2} \tag{26}$$

where I_v^{h} and I_v^{v}, respectively designate the intensity of horizontally and vertically scattered light. For symmetric top molecules, the polarization anisotropy is particularly simple

$$\gamma = (\alpha_{||} - \alpha_{\perp}) \tag{27}$$

Here (||) refers to the parallel and (⊥) to the perpendicular component, such that the average molecular polarizability becomes $\alpha = {}^1/_3(\alpha_{\perp} + 2\alpha_{||})$. Traditionally, α is obtained from refractivities using the appropriate relation from section II. Therefore, for symmetric top molecules, all polarizability components can be determined by combining depolarization and refractivity data.

To avoid reference to more than one type of experiment, we instead computed depolarization ratios directly from our ab initio polarizabilities. Figure 1a displays depolarization ratios derived from HF polarizabilities for various basis sets. Also shown are more recent experimental determinations of ρ_v obtained from Rayleigh scattering measurements on benzene vapor. Comparisons with experiment are relevant only above ∼1.8 eV where nonelectronic contributions to α can be disregarded (to a first approximation). Also, comparisons should not be extended above ∼4.5 eV where the first electronic absorption of benzene originates.

The experimental numbers fall between ρ_v corresponding to the [321/21] basis set on the one side, and the [432/32], Sadlej, and [7643/643] sets on the other side. Judging from ρ_v alone, it is not possible to assess whether the [321/21] or the [432/32] gives the better description. However, we can conclude that the [432/32] set does improve the description of ρ_v relative to the Sadlej set. Also, the larger [7643/643] basis set does not improve the description of ρ_v significantly, justifying our general use of the [432/32] set.

In Figure 1b, depolarization ratios derived for CAS polarizabilities are displayed along with the corresponding uncorrelated numbers. Imposition of the [00002121] CAS causes a small decrease in ρ_v relative to the HF result which, however, increases with frequency. For the [00003231] CAS this effect is more outspoken. Thus, in terms of depolarization ratios, accounting for static correlation alone in fact leads to a poorer description.

VI. Results and Discussion: Refractive Index

Calculation of the refractive index requires information on the density of the phase considered. For the gas phase we used a virial expansion[47] applicable at moderate pressures and temperatures, and for the liquid phase, the tabulated value,[48] $\rho = 0.8765$ g/cm^3 valid at 293.15 K was used. For both phases of benzene, we derived refractivities using eq 25 and eq 22. These apply for isotropic situations only and with vanishing magnetization of the medium. The latter condition we confirmed by computing static magnetizabilities along with the polarizabilities. Quite generally, we observed that these magnetizabilities were three orders of magnitude smaller that the corresponding polarizabilities.

A. Gas Phase of Benzene. Refractivities calculated at 1 bar of pressure and 293.15 K are shown in Figure 2 along with the very sparse experimental data.[49] Not surprisingly at these densities, the classical internal-field correction is without any effect. Regarding the dispersion, the refractivities show a smooth increase with frequency, but begin to diverge around 6.5 eV due to the ($^1A_{1g} \rightarrow {}^1E_{1u}$) transition at 7.43 eV. As seen from Table 9, this dipole transition is the first allowed for D_{2h} symmetry, the two lower being allowed only if mixing of states and coupling to the vibrational subsystem is considered. Although the response formalism does account for dipole forbidden transitions, in terms of excitation energies, the corresponding absorption peaks lack in the dispersion curve for the polarizabilities. In other words, from Table 9 we know that additional peaks around ∼5.8 eV should occur for the dispersion curves in Figure 2, but are absent due to the high symmetry of the benzene molecule. We consider this a serious deficiency of the current approach.

As to the correctness of the refractive indices calculated below frequencies where inelastic light scattering occurs, we have very little experimental work to refer to. To our knowledge only Prytz[49] has measured the refractive index of benzene vapor at ambient conditions. Although close agreement with experiment is seen from Figure 2, no firm conclusion should be based on such sparse data. We therefore urge that more up-to-date measurements be reported.

B. Liquid Benzene. Figure 3 depicts three different approaches to the calculation of the refractive index, differing by

the polarizabilities used in eqs 25 and 22. In Figure 3a, we display results for the refractive index as derived from gas phase polarizabilities. Hence, comparing the refractive index, as derived from either eq 25 or eq 22, quantifies the importance of the Lorentz internal field, for isolated molecules at liquid densities. In contrast, Figure 3b displays the situation where the polarizabilities have been derived using the ISCRF procedure, updating the dielectric constant as $\epsilon = 1 + 4\pi - \langle\alpha\rangle$. Thus, in this approach α_{sol} is derived quantum mechanically, and the internal field neglected in the succesive derivations of the dielectric constant. The results presented in Figure 3c are similar to those of Figure 3b, but differs to the extend that the ISCRF procedure now employs the internal field assumption, that is updating the dielectric constant as $\epsilon = (3 + 8\pi - \langle\alpha\rangle/3 - 4\pi - \langle\alpha\rangle$.

Along with the theoretical refractivities in Figure 3 are experimental refractivities for the IR region as tabulated by Bertie et al.,[50] and for the UV−VIS region as given by the Sellmeier formula.[51] The latter extends to long wavelengths since it accounts for the electronic contributions exclusively, but limited to ~4.5 eV where the first electronic absorption takes place for liquid benzene.[48] Therefore, the difference between these numbers and those of Bertie et al. may be an experimental indication of the importance of nonelectronic contributions to the refractive index. To assess the validity of the Sellmeier formula, comparisons with other observations for the UV−VIS region were made, and the agreement found to be satisfactory.

Focusing on Figure 3a, we see that calculating the refractive index from eq 25 using vacuum polarizabilities, underestimates the experimental results. The traditional remedy is the inclusion of the internal field correction, and from Figure 3a we confirm that this simple correction works quite well, in fact all the way up to 4 eV. At higher frequencies we note that the Lorentz internal-field correction results in an enhanced dispersion, relative to results obtained with eq 25.

Including molecular interactions specifically, using the ISCRF approach, but neglecting internal field effects, underestimates the experimental result, as confirmed from the Figure 3b. If we now include the internal field in the final evaluation of the refractive index, from Figure 3b we observe significantly enhanced refractivities relative to experiment. At high frequencies the dispersion becomes unphysically large, and for the last frequency point we in fact encounter a breakdown of eq 22, i.e., $3 \leq 4\pi - \langle\alpha\rangle$. This is a well-known problem for the Lorenz−Lorentz model for high polarization states of the medium.[2] The divergence of the dispersion in Figure 3b is not caused by lowering of the ($^1A_{1g} \rightarrow {}^1E_{1u}$) transition due to the ISCRF procedure (which would have the same effect) since, otherwise, both curves in Figure 3b would display this feature. Consistent use of the Lorentz internal field and the ISCRF procedure requires consideration of the internal field, both in the updating of ϵ and the evaluation of the refractive index. From Figure 3c it is clear that such an approach leads to a behaviour even worse than that seen in Figure 3b: now the refractive index diverges for the two highest frequency points. Also, from Figure 3c we see that it is the use of eq 22 instead of eq 25 which hampers the description. In fact, using eq 25 underestimates the refractive index, despite that the internal field has been taken into consideration in the ISCRF procedure.

The general conclusion of Figure 3 is that the Lorenz−Lorentz equation, employed with gas phase polarizabilities, gives close agreement with experiment. This illustrates the general and well-known success of eq 22 for describing the refractive index of many nonpolar liquids. Closer inspection of Figure 3a reveals that eq 22 yields refractivities slightly larger than the experimental data. This implies either of the two conditions: either the Lorentz model significantly exaggerates the actual internal field or the specific solvent interactions are negligible or counteract the effect of the internal field. That ISCRF refractivities calculated with eq 25 remain below experiment, while those calculated from eq 22 may become unphysical, indicates that the Lorentz internal-field model is hypersensitive to the polarization state of the medium.

Evidently, our attept at a consistent description of the refractive index, treating the specific molecular interactions quantum mechanically and the screening of the optical field classically, bares little fruit, which we ascribe to the simplicity of the Lorentz model. On the other hand, we have illustrated an iterative use of the MCSCRF method, allowing molecular optical properties to be determined self-consistently, with respect to the corresponding macroscopic properties. Hence, implementing the ISCRF model with more appropriate internal field models seems to be promizing.

VII. Conclusion and Perspective

We have presented a generalization of the classical approach to calculation of refractive indices, thereby allowing us to treat the linear response of any material. Concepts regarding the calculation of refractivities using quantum mechanical models, together with the simple Lorentz internal field model has been discussed. An iterative implementation of the MCSCRF procedure has been devised in order to eliminate reference to the property calculated, as introduced by the internal field model.

The polarization tensor of our model system, benzene, was investigated. We performed a full basis set investigation employing the ANO basis set. From this we conclude that the medium sized basis set [432/32] gives polarizabilities close to the HF-limit with reasonable computational times. Final conclusion could not be reached as to a precise HF-limit for α, but we predict that the calculations with the basis set [7643/643] are close to it. Contrary to previous conclusions we find that with an adequate ANO basis set, electron correlation, calculated using a CAS approach, lowers the polarizability.

The issue of comparing polarizabilities to experimental data was discussed. Comparisons to experimental depolarization ratios are inconclusive concerning the importance of electron correlation and the applicability of the MCSCF method to benzene. Refractive indices for benzene vapour agree well with the very limited experimental data, but problems with describing the correct dispersion appear.

By ISCRF sample computations, we illustrated how specific molecular interactions can be treated quantum mechanically while interactions, as mediated by the optical field, are given a simple classical treatment. Results for the refractive index, as obtained from a consistent use of the ISCRF procedure, are inferior to those obtained with gas phase polarizabilities in the Lorenz−Lorentz equation. This we ascribe to shortcomings in the representation of the internal field in the Lorentz model. Clearly, development of more appropriate internal field models is required along with investigations of the specific nature of the internal field.

Acknowledgment. M.A.R. thanks the ONR chemistry division for support of this work through the CAMP MURI program. He is also grateful for support from the Chemistry Division of the NSF. K.V.M. thanks Statens Naturvidenskabelige Forskningsråd for support.

References and Notes

(1) Mikkelsen, K. V.; Jørgensen, P.; Aagaard Jensen, H. J. *J. Chem. Phys.* **1994**, *100* (9), 6597−6607.

(2) Böttcher, C. J. F. *The Theory of Electric Polarization*; Elsevier: Amsterdam, 1973; Vol. I.

(3) Böttcher, C. J. F.; Bordewijk, P. *The Theory of Electric Polarization*; Elsevier: Amsterdam, 1978; Vol. II.

(4) Wagnière, G. H. *Linear and Nonlinear Optical Properties of Molecules*; Verlag Helvetica Chimica Acta: Basel, 1993.

(5) Lorentz, H A. *Ann. Phys.* **1880**, *9*, 641.

(6) Pietralla, M.; Grossmann, H. P.; Krüger, J. K. *J. Polym. Sci.* **1982**, *20*, 1193−1205.

(7) Lorenz, L. V. *Ann. Phys.* **1880**, *11*, 70.

(8) De Jong, S.; Groeneweg, F.; Van Voorst Vader, F. *J. Appl. Crystallogr.* **1990**, *24*, 171−174.

(9) Wlochowicz, A.; Rabiej, St.; Janicki, J. *Acta Polym.* **1982**, *33* (2), 117−124.

(10) de Vries, H. *Colloid Polym. Sci.* **1979**, *257* (3), 226−238.

(11) Hong, S. D.; Chang, C.; Stein, R. S. *J. Polym. Sci.* **1975**, *13*, 1447−1459.

(12) Proutiere, A.; Megnassan, E.; Hucteau, H. *J. Phys. Chem.* **1992**, *98* (8), 3485−3489.

(13) Wortmann, R.; Bishop, D. M. *J. Chem. Phys.* **1998**, *108*, 1001−1007.

(14) Helgaker, T.; Jensen, H. J. Aa.; Jørgensen, P.; Olsen, J.; Ruud, K.; Ågren, H.; Andersen, T.; Bak, K. L.; Bakken, V.; Christiansen, O.; Dahle, P.; Dalskov, E. K.; Enevoldsen, T.; Fernandez, B.; Heiberg, H.; Hettema, H.; Jonsson, D.; Kirpekar, S.; Kobayashi, R.; Koch, H.; Mikkelsen, K. V.; Norman, P.; Packer, M. J.; Saue, T.; Taylor, P. R.; Vahtras, O. *Dalton: An electronic structure program*, Release 1.0, 1997. http://www.kjemi.uio.no/software/dalton/dalton.html.

(15) Olsen, J.; Jørgensen, P. *J. Chem. Phys.* **1985**, *82* (7), 3235−3264.

(16) Mikkelsen, K. V.; Luo, Y.; Ågren, H.; Jørgensen, P. *J. Chem. Phys.* **1994**, *100* (11), 8240−8250.

(17) Mikkelsen, K. V.; Luo, Y.; Ågren, H.; Jørgensen, P. *J. Chem. Phys.* **1995**, *102* (23), 9362−9366.

(18) Billing, G. D.; Mikkelsen, K. V. *Advances in Molecular Dynamics and Chemical Kinetics*; Wiley: New York, 1997.

(19) Chablo, A.; Hinchliffe, A. *Chem. Phys. Lett.* **1980**, *72* (1), 149−151.

(20) Perez, J. J.; Villar, H. O. *Chem. Phys. Lett.* **1992**, *188* (5,6), 604−608.

(21) Adant, C.; Bredas, J. L.; Dupuis, M. *J. Phys. Chem. A*, **1997**, *101*, 3025−3031.

(22) Perrin, E.; Prasad, P. N.; Mougenot, P.; Dupuis, M. *J. Chem. Phys.* **1989**, *91* (8), 4728−4732.

(23) Archibong, F. E.; Thakkar, A. J. *Mol. Phys.* **1993**, *81* (3) 557−567.

(24) Hinchliffe, A.; Humberto, J.; Soscun, M. *J. Mol. Struct.* **1993**, *300*, 1−7.

(25) Lazzeretti, P.; Malagoli, M.; Zanasi, R. *Chem. Phys. Lett.* **1990**, *17* (1, 2), 101−104.

(26) Lazzeretti, P.; Malagoli, M.; Zanasi, R. *J. Mol. Struct. (Theochem)* **1991**, *234*, 127−145.

(27) Augspurger, J. D.; Dykstra, C. E. *Mol. Phys.* **1992**, *76* (1), 229−237.

(28) Norman, P.; Jonsson, D.; Ågren, H. *Chem. Phys. Lett.* **1997**, *268*, 337.

(29) Stanton, J. F.; Bartlett, R. J. *J. Chem. Phys.* **1993**, *99* (7), 5178−5183.

(30) Karna, S. P.; Gautam, B.; Talapatra; Prasad, P. N. *J. Chem. Phys.* **1991**, *95* (8), 5873−5881.

(31) Lazzeretti, P.; Malagoli, M.; Turci, L.; Zanasi, R. *J. Chem. Phys.* **1993**, *99* (8), 6027−6030.

(32) Widmark, P.-O.; Malmquist, P.-Å.; Roos, B. O. *Theor. Chim. Acta* **1990**, *77*, 291−306.

(33) Widmark, P.-O.; Joakim, P. B.; Roos, B. O. *Theor. Chim. Acta* **1991**, *79*, 419−432.

(34) Almlöf, J.; Taylor, P. R., *J. Chem. Phys.* **1987**, *86* (7), 4070−4077.

(35) Stevens, R. M.; Laws, E. A.; Libscomb, W. N. *J. Am. Chem. Soc.* **1971**, *93*, 2603.

(36) Stoicheff, B. P. *Can. J. Phys.* **1954**, *32*, 339−346.

(37) Cabana, A.; Bachand, J.; Gigúere, J. *Can. J. Phys.* **1974**, *52* (20), 1949−1955.

(38) Sadlej, A. J. *Collect. Czech. Chem. Commun.* **1988**, *53*, 1995−2015.

(39) Packer, M. J.; Dalskov, E. K.; enevoldsen, T.; Jensen, H. J. Aa. *J. Chem. Phys.* **1996**, *105* (14), 5886−5900.

(40) Roos, B. O.; Andersson, K.; Fülscher, M. P. *Chem. Phys. Lett.* **1992**, *192* (1), 5−13.

(41) Malmqvist, P.-Å.; Roos, B. O. *Theor. Chim. Acta* **1992**, *83*, 191−199.

(42) Lorentzon, J.; Malmqvist, P.-Å.; Fülscher, M. P.; Roos, B. O. *Theor. Chim. Acta* **1995**, *91*, 91.

(43) Christiansen, O.; Koch, H.; Halkier, A.; Jørgensen, P.; Helgaker, T.; Sánchez de Merás, A. *J. Chem. Phys.* **1996**, *105* (16), 6921−6939.

(44) Buckingham, A. D.; Pople, J. A. *Proc. Phys. Soc. A*, **1955**, *68*, 905.

(45) Buckingham, A. D.; Pople, J. A. *Proc. Phys. Soc. B*, **1956**, *69*, 1133.

(46) Bridge, N. J.; Buckingham, A. D. *Proc. Roy. Soc. A* **1966**, **295**, 334−348.

(47) Dymond, J. H.; Smith, E. B. *The Virial Coefficients of Pure Gases and Mixtures, A Critical Compilation*; Oxford University Press: Oxford, 1980.

(48) Lide, D. R. *Handbook of Chemistry and Physics*, 73rd Ed.; CRC Press, Inc.: London, 1992−1993.

(49) Prytz, K. *Wiedemanns Ann.* **1980**, *2*, 104−120.

(50) Bertie, J. E.; Norman Jones, R.; Dale Keefe, C. *Appl. Spectrosc.* **1993**, *47* (7), 891−911.

(51) Hellwarth, R. W. *Prog. Quantum. Electron.* **1977**, *5*, 1−68.

(52) Herzberg, G. *Molecular Spectra and Molecular Structure*; D. Van Nostrand Company, Inc.: New York, 1966.

(53) Hiraya, A.; Shobatake, K. *J. Chem. Phys.* **1991**, *94* (12), 7700−7706.

(54) Alms, G. R.; Burnham, A. K.; Flygaare, W./ H. *J. Chem. Phys.* **1975**, *63* (8), 3321−3326.

(55) Bogaard, M. P.; Buckingham, D.; Pierens, R. K.; White, A. H. *Chem. Soc., Faraday Trans. 1* **1978**, *74*, 3008−3015.

(56) Panachev, F. I.; Korableva, E. Yu.; Shakhparonov, M. I. *Russ. J. Phys. Chem.* **1976**, *50* (7), 1130.

(57) In the derivation of eq 14 it is assumed that $\chi \leq 1$ which for most dense media is fulfilled, such that $(1 + x)^{-1} = 1 + x^2 + x^3 + ...$ is valid. Alternatively, eq 14 follows directly from eq 10 if this equation is taken as the definition of the internal field i.e.; $\mathbf{E}_{\text{int}} = \mathbf{E} + \mathbf{LP}$.

(58) Such numbers are found on page 288, Table 38 in ref 3.